

## General Disclaimer

### One or more of the Following Statements may affect this Document

- This document has been reproduced from the best copy furnished by the organizational source. It is being released in the interest of making available as much information as possible.
- This document may contain data, which exceeds the sheet parameters. It was furnished in this condition by the organizational source and is the best copy available.
- This document may contain tone-on-tone or color graphs, charts and/or pictures, which have been reproduced in black and white.
- This document is paginated as submitted by the original source.
- Portions of this document are not fully legible due to the historical nature of some of the material. However, it is the best reproduction available from the original submission.

**NASA Technical Memorandum 78943**

(NASA-TM-78943) SOME FLOW PHENOMENA IN A  
CONSTANT AREA DUCT WITH A BORDA TYPE INLET  
INCLUDING THE CRITICAL REGION (NASA) 14 p  
HC A02/MF A01 CSCL 20D

N78-27367

Unclas  
25211

g3/34

**SOME FLOW PHENOMENA IN A CONSTANT  
AREA DUCT WITH A BORDA TYPE INLET  
INCLUDING THE CRITICAL REGION**

by R. C. Hendricks and R. J. Simoneau  
Lewis Research Center  
Cleveland, Ohio



**TECHNICAL PAPER to be presented at the  
Winter Annual Meeting  
sponsored by the American Society of Mechanical Engineers  
San Francisco, California, December 10-15, 1978**

# SOME FLOW PHENOMENA IN A CONSTANT AREA DUCT WITH A BORDA TYPE INLET INCLUDING THE CRITICAL REGION

R. C. Hendricks and R. J. Simoneau  
National Aeronautics and Space Administration  
Lewis Research Center  
Cleveland, Ohio

## ABSTRACT

Mass limiting flow characteristics for a 55 L/D tube with a Borda type inlet have been assessed over large ranges of temperature and pressure ( $0.68 \leq T/T_c \leq 2.3$ ;  $P/P_c \leq 3$ ) using fluid nitrogen ( $T_c = 126.3$  K,  $P_c = 3.417$  MPa). Under certain conditions, separation and pressure drop at the inlet was sufficiently strong to permit partial vaporization and the remaining fluid flowed through the tube as if it were a free jet. An empirical relation was determined which defines conditions under which this type of flow can occur. A flow coefficient is presented which enables one to estimate flow rates over the experimental range. A flow rate stagnation pressure map for selected stagnation isotherms and pressure profiles document these flow phenomena.

## INTRODUCTION

Flow separation represents a divergence of streamlines from a bounding surface and may or may not be accompanied by a free interface. It represents a common event in fluid dynamics. Airfoils are highly susceptible to separation whether an element of a power system such as a compressor or turbine or an aerodynamic surface of a wing or empennage. In such components separation is undesirable. However in fluid dynamic controls, separation is used advantageously. In fluid circuit logic, separation is used to switch power circuits; in flight, spoilers rapidly decrease lift; and in seals, separation can assist in controlling the loss of the working fluid.

In internal flows, one of the most common inlets is sharp edged. However, the inlet most susceptible to separation is the Borda tube. In either case, a vena-contracta is formed and the region of detachment

depends on fluid conditions. If the fluid has the potential to vaporize under these circumstances, the problem is substantially more complicated.

While many texts and papers deal with such inlet phenomena, few have addressed the problem of entrance effects on two phase choked flows (1-6) and one addresses the effects at very large L/D (7).

In engineering applications, it is customary to arbitrarily assign a friction factor (L/D) equivalent to account for entrance losses. While this is entirely justified in many problems, it is not for sealing surfaces. In high performance seals, the entrance effects and associated zones of separation cannot be ignored or arbitrarily assigned for they play a major role in seal dynamics; as will be established, entrance conditions can control mass flow and establish pressure distributions for mass limiting flows.

While the material discussed herein is germane to all of the above fields and to separation phenomena, it is primarily applicable to fluid control and dynamics of sealing surfaces. Thus the purpose of this paper is to present flow rate and axial pressure profile data established by mass limiting flows through a 55 L/D straight tube with a Borda type inlet over a large range of stagnation temperatures and pressures including the critical region.

## APPARATUS AND INSTRUMENTATION

The basic flow facility was of the blowdown type and is described in detail in Ref. 8. A photograph of the installed test section (fig. 1) illustrates the pressure taps and associated plumbing. The flow was upward, around the U and downward through the test section. The flow rates were metered using a venturi flowmeter located in the bottom of the storage

tank. Inlet stagnation conditions were measured in the mixing chamber shown immediately behind the scale in Fig. 1.

The 55 L/D straight 0.483 cm diameter tube test section consisted of two parts, the Borda type inlet and a straight tube with a 7° diffuser (see figs. 1 and 2). A photograph of the Borda type inlet is shown in Fig. 3. While not a true Borda inlet, the flow must still experience a reversal prior to entering the test section.

Eighteen local pressure taps, three stagnation pressures, and a backpressure were used to establish the axial pressure profiles. The tap locations are given in Table I.

The parameters were monitored using a mini-computer-CRT display at 1/2-second update intervals until all conditions appeared satisfactory. At that time the signals were digitized, recorded, and subsequently reduced using the LeRC data acquisition system. While the accuracy of the static transducers was limited to 1/2 percent and the range was large, systematic calibration and subsequent checks with higher sensitivity differential pressure transducers indicated a relative difference of 0.1 percent could be established and reproduced.

#### FLOW MODEL AND DISCUSSION

The type of separation phenomena encountered herein results from a discontinuity in the shape of the bounding surface. The theoretical inviscid streamlines conform to the bounding surface. No such conformation to the surface exists with the viscous flow and separation is initiated. Growth or decay of this separation, or perturbation, depends on the degree of the discontinuity. The true Borda inlet causes a full reversal of the streamline at the inlet and represents the strongest degree of discontinuity for simple geometries. As such, the incompressible contraction coefficient<sup>1</sup> of 0.5 (9) represents the most severe separation phenomenon for simple tube inlets.

The geometry of the free streamline in potential flow is found by integrating the real and imaginary components of  $dz$  (10) (see fig. 4).

$$z = X + iY = \frac{1}{V_0} \int V_0 \frac{dz}{dw} dw \quad (1)$$

The free streamline can be defined in terms of the parameter  $\theta$ , where  $\theta$  ranges from 0 to  $\pi$ :

$$x_0 = \frac{2X}{B} = -\frac{1}{\pi} \left\{ \sin^2\left(\frac{\theta}{2}\right) + \log \left[ \cos\left(\frac{\theta}{2}\right) \right] \right\} \quad (2)$$

$$y_0 = \frac{4Y}{B} = \frac{1}{\pi} (2\pi - \theta + \sin \theta) \quad (3)$$

While the above applies to the two-dimensional case (fig. 4(a)), it can be shown that similar streamlines exist for the axisymmetric case (10), and the contraction area or contraction coefficient is still 0.5;  $A_2/A_1 = 1/2$  (fig. 4(b)), see Ref. 9.

Although the focus of this paper is to provide characteristic flow and pressure profile data for a Borda inlet, a model of the flow phenomena is suggested in an attempt to explain the major experimen-

<sup>1</sup>For a channel or slot, the ratio of flow width to channel width; for a tube,  $A_2/A_1$ , flow area to tube area.

tal findings. A sketch of this model is shown as Fig. 5.

(1) The entrance contraction is sufficiently strong to cause separation and vaporization, that is, the radial velocity is significant and forces separation resulting in the free streamline some distance from the wall.

(2) The entrance vortex zone, 2 to 4 diameters in length, appears to always exist setting up an initial recompression zone.

(3) Under certain conditions (low temperature, high pressure fluid) the entrance vortex is sufficiently weak and initiates partial recompression; usually this recompression is only to the saturation pressure<sup>5</sup>. The fluid jet then traverses the tube length with only a small pressure rise.

(4) For the free jet conditions, the vapor and/or boundary layer growth is assumed to form a diffuser. This zone may extend through the tube or may not exist at all.

(5) Strong recompression in the secondary zone can occur within the tube due to transition or be forced on the flow by adjusting the backpressure. This zone may not exist within the 55 L/D or it may intersect the initial recompression zone.

(6) Metastable states and normal states of condensation and vaporization are assumed to occur.

#### RESULTS AND DISCUSSION

##### Pressure Profiles

Typical axial pressure profiles for the 55 L/D tube with Borda inlet are illustrated as Figs. 6 and 7. For reference purposes, a typical pressure profile for the gaseous state is given on Fig. 6. Except for the abrupt nearly two to one characteristic drop at the inlet followed by recompression, it appears as a standard friction profile for a tube.

Holding inlet stagnation conditions nearly constant while the backpressure is varied results in the family of profiles displayed on Fig. 6. At a backpressure of 1.69 MPa (245 psia), the pressure profile near the exit appears monotonic increasing. This is a transition point which signals that secondary recompression is now within the tube. Further increases in backpressure move the secondary recompression zone further into the tube until at sufficiently high backpressures the system finally becomes unchoked. Profiles as run 1160 are very difficult to obtain by varying the backpressure. Secondary recompression within the duct is most easily established by changing stagnation conditions. In Fig. 7, recompression is effected along the 117 K isotherm by decreasing the stagnation pressure from 7.28 MPa (1055 psia) to 5.93 MPa (860 psia). At 7.28 MPa (1055 psia) the initial recompression is to about 1.48 MPa (215 psia) followed by the characteristic monotonic rise in pressure to the exit in the characteristic diffuser zone (fig. 5).

At 6.79 MPa (985 psia), the secondary recompression zone is within the tube and at 5.97 MPa (865 psia) the zone has moved near the initial recompression zone; note that when the two recompression zones merge, the initial recompression recovery pressure equals that of the secondary recompression zone, that is, more characteristic of the gas profile. One should note that once transition has occurred, all profiles merge into a single profile downstream of

<sup>2</sup>The stagnation temperature usually tends to increase over the course of a run due to heating by the pressurizing gas.

<sup>3</sup>Based on inlet stagnation conditions.

of the transition point for a given isotherm.

Secondary recompression can be made to take place within the tube by varying the stagnation temperature along an isobar. Along the 10.45 MPa (1515 psia) isobar at 121.7 K, the zone of secondary recompression is greater than 55 L/D, that is, beyond the tube exit, even though the temperature is close to critical. The initial zone of recompression is to about 1.62 MPa (235 psia), followed by the characteristic monotonic rise in pressure through the characteristic diffuser zone. At 127.8 K, which is greater than the critical temperature ( $T_c = 126.3$  K), the zone of secondary recompression is within the tube. The initial recompression pressure is to about 2.03 MPa (295 psia). At 130.5 K, the zone has moved further toward the inlet while the pressure in the initial recompression zone has increased to about 2.24 MPa (325 psia). It would appear that the jet cannot be sustained for conditions close to the thermodynamic critical point for 55 L/D. This does not mean that lesser L/D could or could not sustain a jet. In either case, the major control is still near the inlet. To illustrate the magnitude of the pressure effect, inlet stagnation conditions where  $P_r = 3.1$  and  $T_r = 0.68$  results in a reduced pressure in the initial recompression zone of 0.0242 and an average diffuser zone reduced pressure of 0.0585. This represents pressure ratios of 128:1 and 53:1, respectively. Such pressure changes can effect serious instabilities in seals, rotor dynamics, and heat exchangers alike.

One of the major questions now becomes: Is there a way to predict the conditions under which the zone of secondary recompression will occur within the tube? Theoretically not at this time, but empirically an expression was determined as illustrated in Fig. 8. For the inlet stagnation conditions less than this locus, secondary recompression does not occur within the 55 L/D tube.

For conditions, above the locus, secondary recompression will occur somewhere within the 55 L/D tube.

An empirical expression for this locus in the present experiment is:

$$P_r = C T_r^7 \quad (4)$$

where

$$C_1(L/D, \epsilon) = 3.6 \quad (5)$$

Equations (4) and (5) are written in the above form because it is expected that the constant  $C_1$  depends on the total tube L/D, which in this case was 55, and surface roughness  $\epsilon$ . For these tests the tube was smooth honed with emery paper.

#### Flow Rate

Reduced flow rate data as a function of reduced stagnation pressure for selected isotherms are given as Fig. 9. Attempts to predict these flow rates theoretically were unsuccessful, so the authors resorted to standard flow coefficient techniques. By calculating the isentropic nonequilibrium two-phase choked flow rate according to the model of Henry and Fauske<sup>4</sup> (11), one can define a flow coefficient as:

$$C_0(P_r, T_r) = \frac{G_{data}/G^*}{G_I/G^*} = \frac{G_r}{G_{rI}} \quad (6)$$

As can be seen from Fig. 10, the coefficient of

<sup>4</sup>Charts of the ideal isentropic flows are available in Ref. 12.

Eq. (6) is strongly dependent on reduced temperature, increasing from about 0.54 at  $T_r = 0.67$  to 0.8 at  $T_r = 1.2$ ; its value then decreases to 0.73 for the gas. Further, it is weakly dependent on pressure away from the saturation locus. At the saturation locus the nonequilibrium model predicts  $C_0$  values less than the locus of Fig. 10, see isolated points of Fig. 9, which may be two phase. Between  $T_r = 0.9$  and 1.0, the data appear to reach a plateau followed by an abrupt rise.

So by calculating the isentropic flow rate using the nonequilibrium model and applying the flow coefficient (fig. 10), the flow rate for this configuration can be determined at any temperature or pressure including the critical region.

While the effect of secondary recompression on the pressure profiles is very significant, little change in the flow rate can be found using Eq. (6) and comparing data with the theoretical curves of Ref. 12. This, of course, implies that the mass limiting effect occurs at the inlet, not at the exit.

Fluid properties for evaluating  $G_{rI}$  were obtained using the computer code established in Ref. 13.

#### SUMMARY

Some flow characteristics in a constant area duct with a Borda type inlet, as may be found in some seals applications and boilers, have been assessed over a wide range of temperature and pressure ( $0.68 \leq T/T_c \leq 2.3$ ;  $P/P_c \leq 3$ ) with fluid nitrogen. ( $T_c = 126.3$  K,  $P_c = 3.417$  MPa). The 55 L/D test section with Borda inlet has a 7° diffuser at the exit.

Under certain conditions, separation at the inlet was sufficiently strong to permit the fluid to flow through the tube as if it were a free jet; in these cases, the diffuser zone extended to the physical diffuser and secondary recompression did not occur within the tube. Otherwise some combination of the initial recompression - diffuser - secondary recompression zones occurred within the tube. In the critical region the diffuser zone vanishes. An empirical criterion was established to determine when secondary recompression would occur within the tube.

The flow coefficient ( $G_r/G_{rI}$ ) varied nonlinearly with temperature from 0.54 at  $T/T_c = 0.68$  to 0.8 at  $T/T_c = 1.5$  to 0.73 for the gas ( $T/T_c = 2.3$ ). The coefficient is weakly dependent on pressure except near saturation where the coefficient tends to unity. Moreover, at a reduced stagnation pressure  $P/P_c = 3.1$  and reduced temperature of 0.68 the average axial reduced pressure was 0.0585, over a 50:1 change. The ratio of the stagnation pressure to the initial recompression zone pressure was over 125:1.

Flow rates for selected isotherms and pressure profiles are presented for this configuration to document these flow phenomena.

#### SYMBOLS

- A area, cm<sup>2</sup>
- B slot or channel width, cm
- $C_1$  constant of Eq. (5)
- $C_0$  flow coefficient, Eq. (6)
- D tube diameter, cm
- G flow rate, g/cm<sup>2</sup>-s

$G_r$  reduced flow rate  
 $G^*$  flow normalizing parameter,  $\sqrt{P_c \rho_c / Z_c}$ ,  
 6010 g/cm<sup>2</sup>-s, for nitrogen  
 $L$  tube length, cm  
 $P$  pressure, MPa  
 $P_r$  reduced pressure,  $P/P_c$   
 $R$  gas constant, MPa-cm<sup>3</sup>/g-K  
 $T$  temperature, K  
 $T_r$  reduced temperature,  $T/T_c$   
 $V$  specific volume, cm<sup>3</sup>/g  
 $V_0$  velocity parameter  
 $w$  complex potential  
 $X$  distance, cm  
 $x_0$  dimensionless distance  
 $Y$  distance, cm  
 $Y_0$  dimensionless distance  
 $Z$  compressibility,  $PV/RT$   
 $z$  complex coordinate, cm  
 $\theta$  parameter  
 $\rho$  density, g/cm<sup>3</sup>  
 $\epsilon$  surface roughness ratio  
 $\delta$  boundary layer thickness, cm

Subscripts:

$c$  critical  
 $I$  isentropic  
 $0$  stagnation

REFERENCES

1 Simoneau, R. J., "Maximum Two-Phase Flow Rates of Sub-Cooled Nitrogen Through a Sharp-Edged Orifice," Advances in Cryogenic Engineering, Vol. 21, Timmerhaus, K. D., and Weitzel, D. H., eds., Plenum Press, New York, 1975, pp. 299-306.  
 2 Richards, R. J., Jacobs, R. B., and Pestalozzi, W. J., "Measurement of the Flow of Liquefied Gases with Sharp-Edged Orifices," Advances in Cryogenic Engineering, Vol. 4, Timmerhaus, K. D., ed., Plenum Press, New York, 1960, pp. 272-285.  
 3 Brennan, J. A., "A Preliminary Study of the Orifice Flow Characteristics of Liquid Nitrogen and Liquid Hydrogen Discharging Into a Vacuum," Advances in Cryogenic Engineering, Vol. 9, Timmerhaus, K. D., ed., Plenum Press, New York, 1964, pp. 292-303.

4 Bonnet, F. W., "Critical Two-Phase Flow of Nitrogen and Oxygen Through Orifices," Advances in Cryogenic Engineering, Vol. 12, Timmerhaus, K. D., ed., Plenum Press, New York, 1967, pp. 427-437.

5 Hesson, J. C., and Peck, R. E., "Flow of Two-Phase Carbon Dioxide," American Institute of Chemical Engineers Journal, Vol. 4, No. 2, 1958, pp. 207-210.

6 Uchida, H., and Nariai, H., "Discharge of Saturated Water Through Pipes and Orifices," Proceedings of the Third International Heat Transfer Conference, American Institute of Chemical Engineers, Vol. 5, 1966, pp. 1-12.

7 Hendricks, R. C., and Simoneau, R. J., "Two-Phase Choked Flow in Tubes With Very Large L/D," Advances in Cryogenic Engineering, Vol. 23, Timmerhaus, K. D., ed., Plenum Press, New York, 1977, pp. 265-275.

8 Hendricks, R. C. et al., "Experimental Heat-Transfer Results For Cryogenic Hydrogen Flowing in Tubes at Subcritical and Supercritical Pressures to 800 Pounds Per Square Inch Absolute," NASA TN D-3095, 1968.

9 Birkhoff, G., and Zarantonello, E. H., Jets, Wakes, and Cavities, Applied Mathematics and Mechanics, Vol. II, Academic Press, New York, 1957.

10 Gurevich, M. I., Theory of Jets in Ideal Fluids, Academic Press, New York, 1965.

11 Henry, R. E., and Fauske, H. K., "The Two-Phase Critical Flow of One-Component Mixtures in Nozzles, Orifices, and Short Tubes," Transactions of the American Society of Mechanical Engineers, Journal of Heat Transfer, Vol. 93, May 1971, pp. 179-187.

12 Simoneau, R. J., and Hendricks, R. C., "Generalized Charts for Computation of Two-Phase Choked Flow of Simple Cryogenic Liquids," Cryogenics, Vol. 17, Feb. 1977, pp. 73-76.

13 Hendricks, R. C., Baron, A. K., and Peller, I. C., "GASP: A Computer Code for Calculating the Thermodynamics and Transport Properties for Ten Fluids: Parahydrogen, Helium, Neon, Methane, Nitrogen, Carbon Monoxide, Oxygen Fluorine, Argon and Carbon Dioxide," NASA TN D-7808, 1975.

TABLE I. - PRESSURE TAP LOCATIONS FOR 55 L/D TUBE WITH BORDA TYPE INLET (SEE FIG. 2)

Pressure tap	Location		Pressure tap	Location	
	cm	in.		cm	in.
$P_0$	Mixing chamber		$P_{10}$	-2.5	-1
$P_{01}$	Line at top of U		$P_{11}$	-1.3	-.5
			$P_{12}$	.64	-.125
$P_{02}$	<sup>a</sup> 25.1	<sup>a</sup> -9.87	$P_{13}$	-.32	-.125
	$P_1$	-26.6	-10.40	$P_{14}$	.32
$P_2$	-26	-10.73	$P_{15}$	.64	.25
$P_3$	-24.5	-9.65	$P_{16}$	1.3	.5
$P_4$	-17.8	-7	$P_{17}$	2.5	1
$P_5$	-15.2	-6	$P_{18}$	5.1	2
$P_7$	-10.2	-4	$P_{back}$	Immediately upstream of backpressure control valve	
$P_8$	-7.6	-3			
$P_9$	-5.1	-2			

<sup>a</sup>At Borda inlet.

ORIGINAL PAGE IS  
OF POOR QUALITY

D-2690

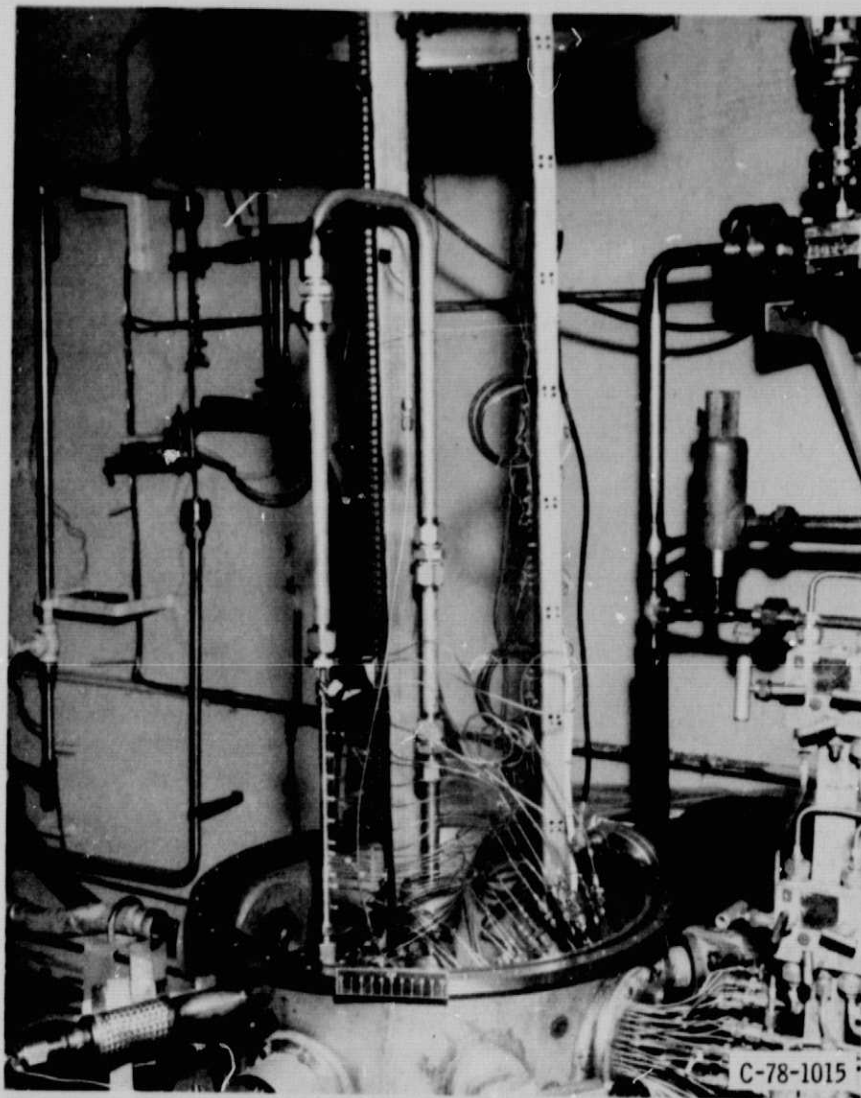
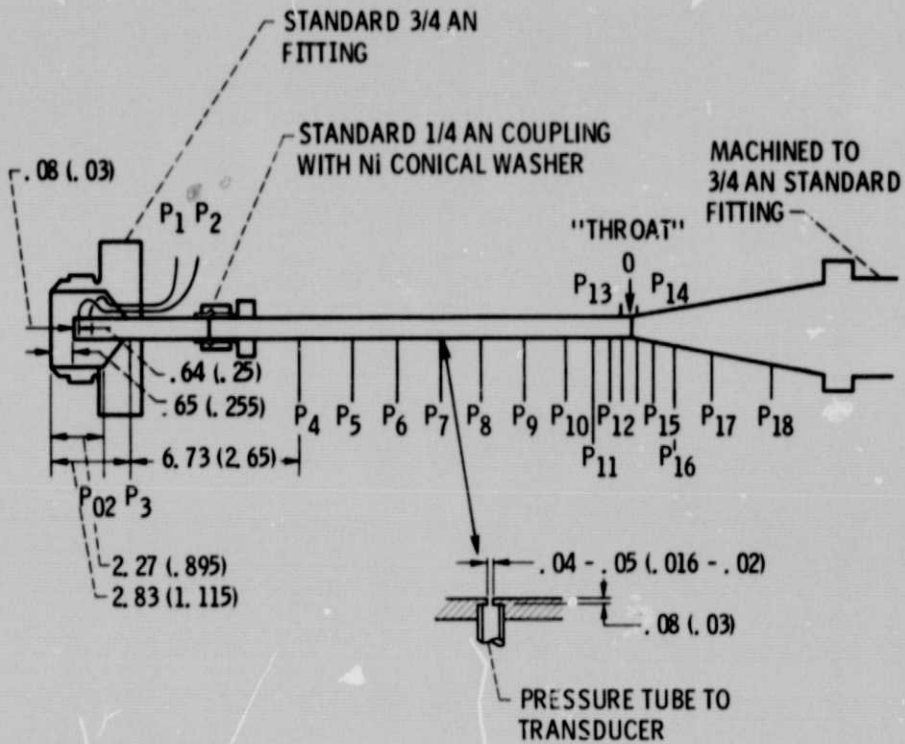


Figure 1. - Apparatus.

ORIGINAL PAGE IS  
OF POOR QUALITY.





TYPICAL PRESSURE TUBE INSTALLATION

Figure 2 - Schematic of 55L/D test section with borda type inlet. See table I for pressure tap locations.



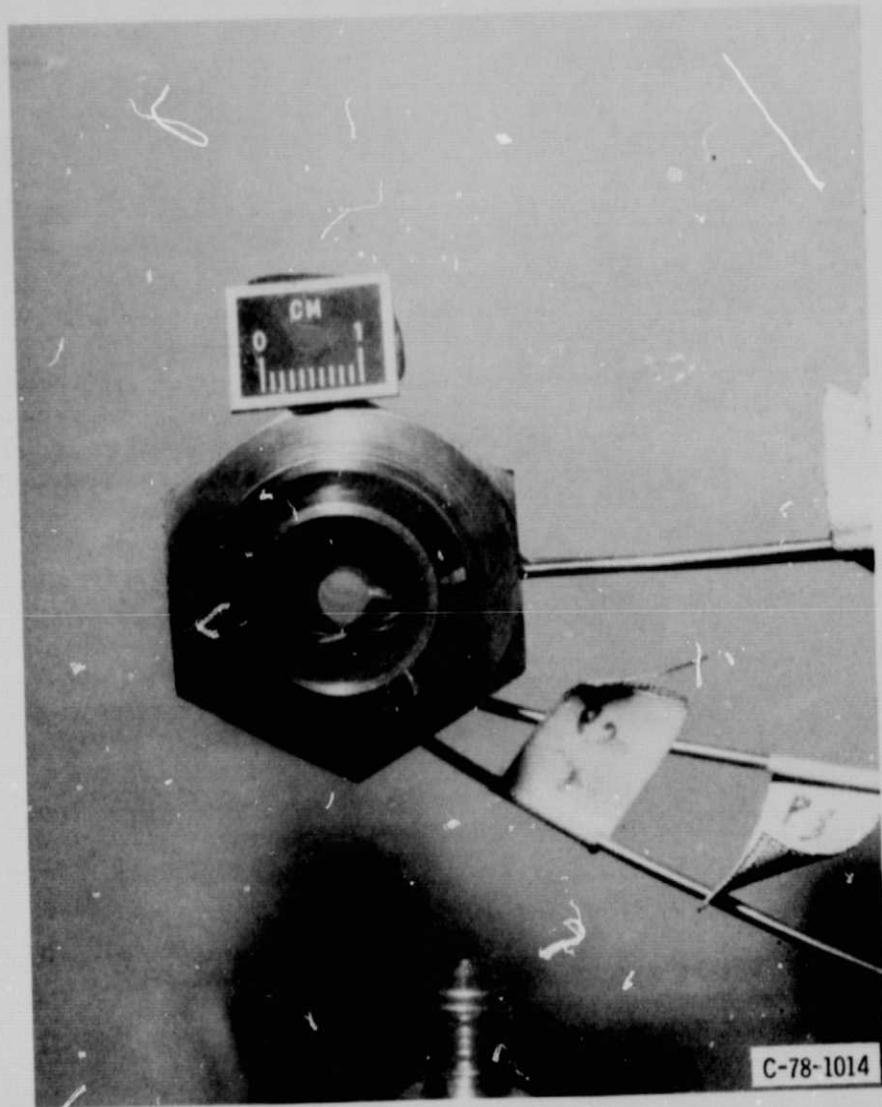


Figure 3. - Borda inlet.

ORIGINAL PAGE IS  
OF POOR QUALITY

IE-7670

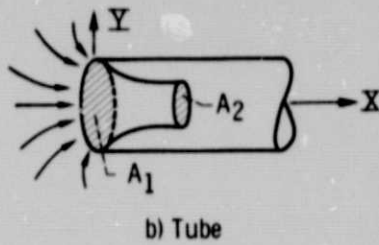
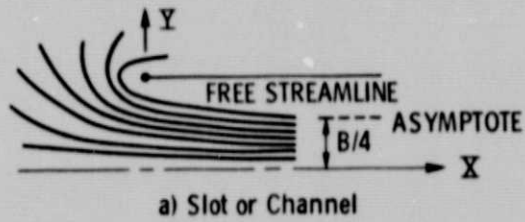


Figure 4. - Schematic for theoretical streamlines for a borda inlet.

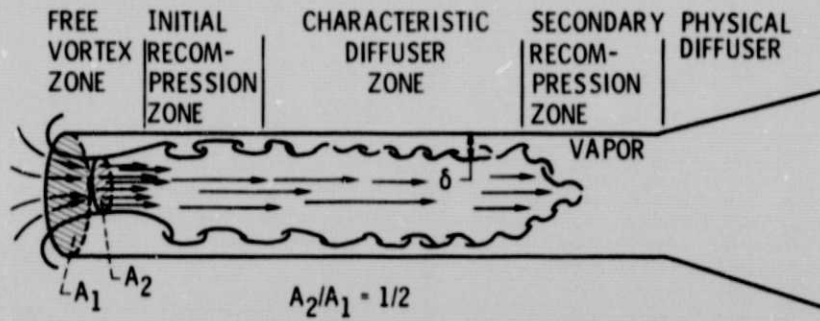


Figure 5. - Suggested model for 55 L/D straight tube with borda type inlet.

3-1670

	$\omega$ g/S	$P_{O_2}$ MPa	$P_{O_2}$ psia	$T_0$ K	RUN	
$\Delta$	727	3.63	527	88.9	1307	
$\triangle$	723	3.61	524	89.2	1308	
$\circ$	721	3.61	523	89.5	1309	
$\square$	719	3.59	521	90.4	1310	
$\triangle$	715	3.59	521	91.4	1311	
$\circ$	699	3.61	524	93.5	1312	
$\nabla$	281	4.64	672	281	1066	GAS

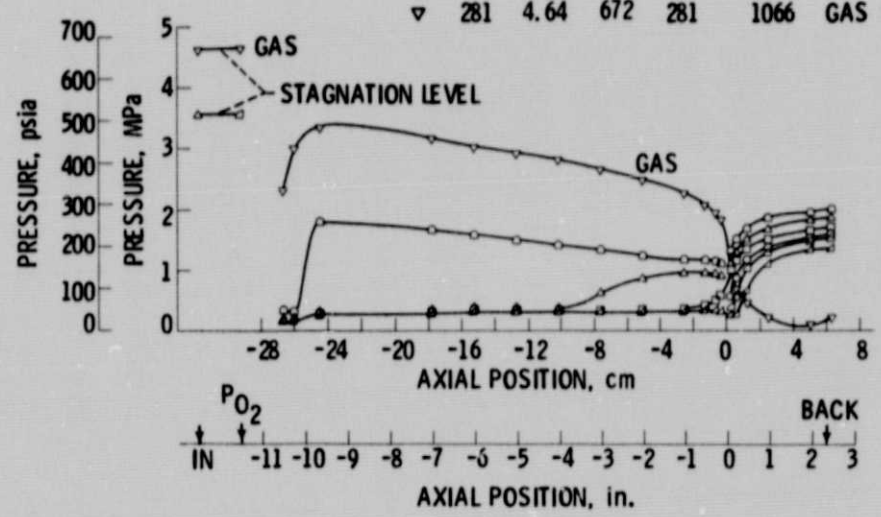


Figure 6. - Typical pressure profiles - axial position 55 L/D straight tube with Borda inlet.

ORIGINAL PAGE IS  
OF POOR QUALITY

	$\dot{w}$ q/S	$P_0$ MPa	$P_0$ psia	$T_0$ K	RUN
▽	1025	10.54	1528	130.5	1302
△	1052	10.45	1515	127.8	1256
□	1122	10.43	1512	121.7	1294
□	821	6.02	873	116.8	1161
○	893	6.90	1000	117.0	1160
△	929	7.32	1062	116.0	1159
△	1259	10.13	1469	86.2	1249

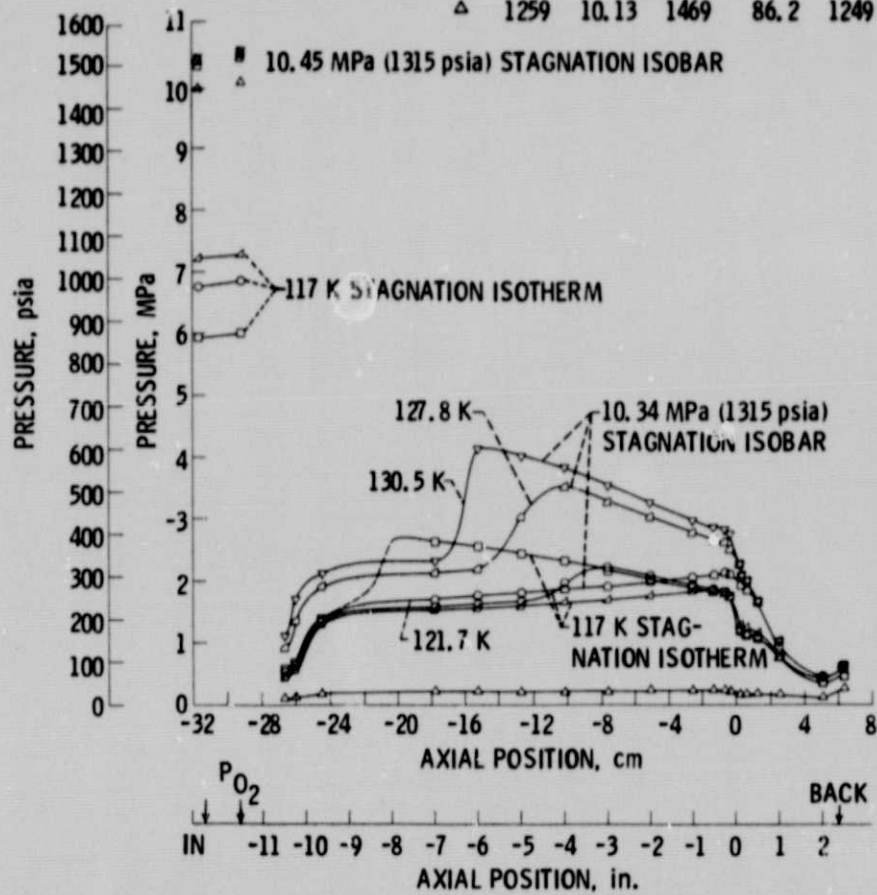


Figure 7. - Typical pressure profiles - axial position 55 L/D straight tube with Borda inlet.

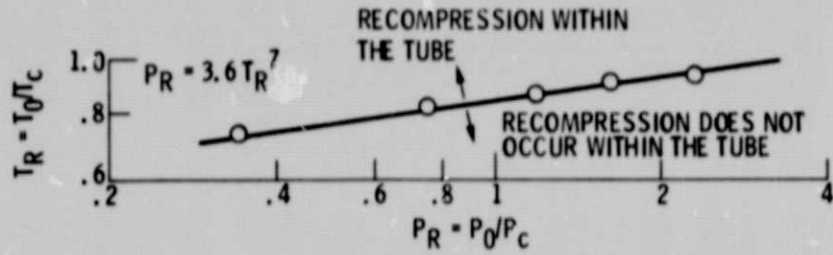


Figure 8. - Flow transition region as a function of reduced pressure and temperature for Borda inlet  $\approx 55$  L/D straight tube -  $T_R \leq 1$ . Fluid nitrogen.

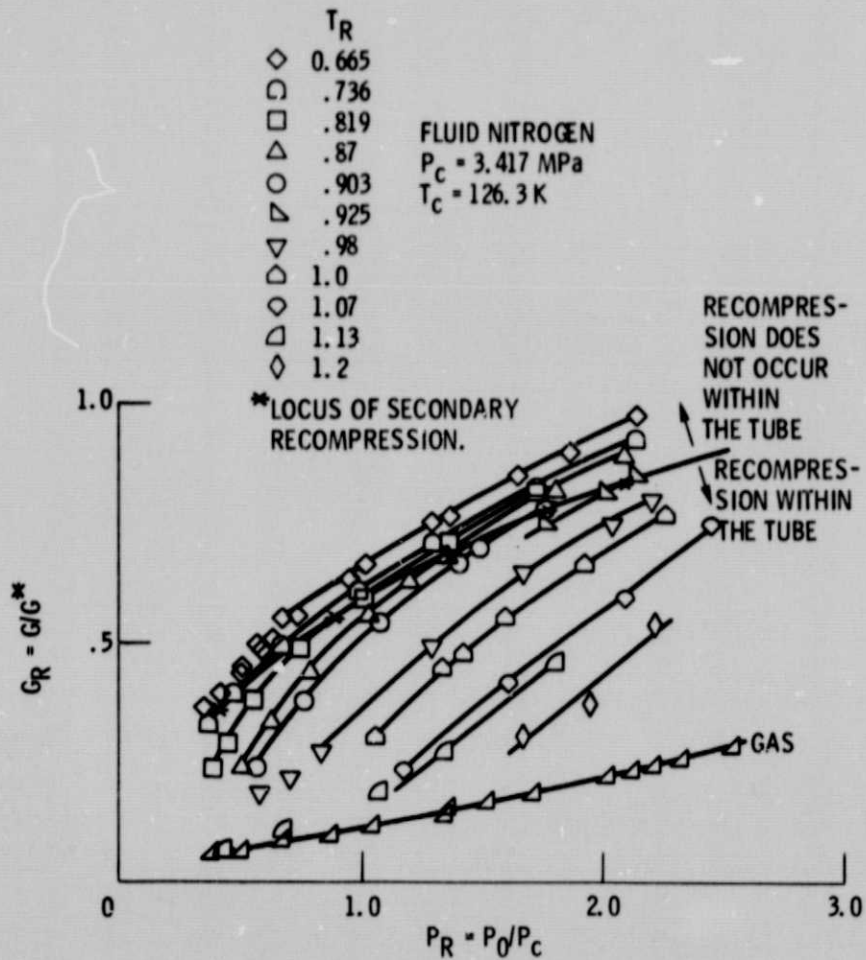


Figure 9. - Reduced flow rate as a function of reduced pressure for selected isotherms. Borda inlet  $\approx 55$  L/D straight tube.

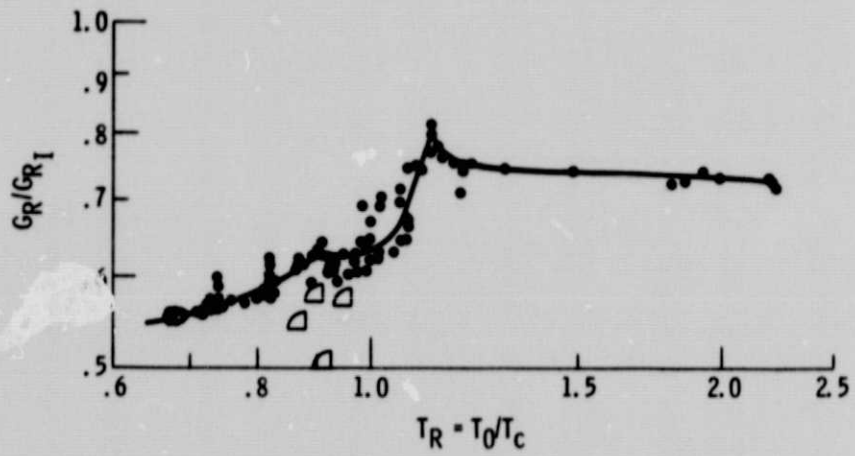


Figure 10. - Reduced flow rate ratio versus reduced temperature for 55 L/D straight tube with a Borda inlet. Fluid nitrogen. ( $\square$ - two phase).



1. Report No. <b>NASA TM-78943</b>	2. Government Accession No.	3. Recipient's Catalog No.	
4. Title and Subtitle <b>SOME FLOW PHENOMENA IN A CONSTANT AREA DUCT WITH A BORDA TYPE INLET INCLUDING THE CRITICAL REGION</b>		5. Report Date	
		6. Performing Organization Code	
7. Author(s) <b>R. C. Hendricks and R. J. Simoneau</b>		8. Performing Organization Report No. <b>E-9690</b>	
9. Performing Organization Name and Address <b>National Aeronautics and Space Administration Lewis Research Center Cleveland, Ohio 44135</b>		10. Work Unit No.	
		11. Contract or Grant No.	
12. Sponsoring Agency Name and Address <b>National Aeronautics and Space Administration Washington, D.C. 20546</b>		13. Type of Report and Period Covered <b>Technical Memorandum</b>	
		14. Sponsoring Agency Code	
15. Supplementary Notes			
16. Abstract <p>Mass limiting flow characteristics for a 55 L/D tube with a Borda type inlet have been assessed over large ranges of temperature and pressure (<math>0.68 \leq T/T_c \leq 2.3</math>; <math>P/P_c \leq 3</math>) using fluid nitrogen (<math>T_c = 126.3 \text{ K}</math>, <math>P_c = 3.417 \text{ MPa}</math>). Under certain conditions, separation and pressure drop at the inlet was sufficiently strong to permit partial vaporization and the remaining fluid flowed through the tube as if it were a free jet. An empirical relation was determined which defines conditions under which this type of flow can occur. A flow coefficient is presented which enables one to estimate flow rates over the experimental range. A flow rate stagnation pressure map for selected stagnation isotherms and pressure profiles document these flow phenomena.</p>			
17. Key Words (Suggested by Author(s)) <b>Fluid flow; Fluid jets; Fluid mechanics; Flow measurements; Flow coefficients</b>		18. Distribution Statement <b>Unclassified - unlimited STAR Category 34</b>	
19. Security Classif. (of this report) <b>Unclassified</b>	20. Security Classif. (of this page) <b>Unclassified</b>	21. No. of Pages	22. Price*